Brief Communications

Cannabinoids Excite Circadian Clock Neurons

Claudio Acuna-Goycolea,[1] Karl Obrietan,[2] and Anthony N. van den Pol[1]

[1]Department of Neurosurgery, Yale University School of Medicine, New Haven, Connecticut 06520, and [2]Department of Neurobiology, Ohio State University, Columbus, Ohio 43210

Cannabinoids, the primary active agent in drugs of abuse such as marijuana and hashish, tend to generate a distorted sense of time. Here we study the effect of cannabinoids on the brain's circadian clock, the suprachiasmatic nucleus (SCN), using patch clamp and cell-attached electrophysiological recordings, RT-PCR, immunocytochemistry, and behavioral analysis. The SCN showed strong expression of the cannabinoid receptor CB1R, as detected with RT-PCR. SCN neurons, including those using GABA as a transmitter, and axons within the SCN, expressed CB1R immunoreactivity. Behaviorally, cannabinoids did not alter the endogenous free-running circadian rhythm in the mouse brain, but did attenuate the ability of the circadian clock to entrain to light zeitgebers. In the absence of light, infusion of the CB1R antagonist AM251 caused a modest phase shift, suggesting endocannabinoid modulation of clock timing. Interestingly, cannabinoids had no effect on glutamate release from the retinohypothalamic projection, suggesting a direct action of cannabinoids on the retinohypothalamic tract was unlikely to explain the inhibition of the phase shift. Within the SCN, cannabinoids were excitatory by a mechanism based on presynaptic CB1R attenuation of axonal GABA release. These data raise the possibility that the time dissociation described by cannabinoid users may result in part from altered circadian clock function and/or entrainment to environmental time cues.

Introduction

The hypothalamic suprachiasmatic nucleus (SCN) receives direct synaptic input from the retina (Moore and Lenn,1972), and serves as the master circadian oscillator in the brain that keeps 24 h time, and drives and orchestrates circadian rhythms throughout both the CNS and peripheral organ systems. A large number of neuroactive transmitters are found in the SCN (van den Pol and Tsujimoto,1985), and many of these influence clock function. Within this context, cannabinoid receptor 1 (CB1R) axonal immunoreactivity has been reported in the medial hypothalamus, including the SCN (Wittmann et al., 2007). Cannabinoids are the major psychotropic/ psychoactive components of marijuana and hashish, and, given that cannabinoids also tend to generate a distorted sense of time (Tinklenberg et al., 1976), it is reasonable to posit that some of the effects of cannabinoids on time perception could be due to modulation of the brain's circadian clock neurons. In line with this idea, a recent study reported that the CB1R agonist CP55940 attenuated a light-induced clock phase advance in hamsters (Sanford et al., 2008), and endogenous cannabinoids show a diurnal variation in the brain (Valenti et al, 2004). However, the mechanisms underlying such behavioral actions of cannabinoids remain obscure.

Here, we examined the effect of cannabinoids on circadian rhythms, and on light-induced clock phase changes in mice. We also studied the expression of the cannabinoid receptor in the SCN with RT-PCR and immunocytochemistry. Finally, as actions of cannabinoids have not been studied at the cellular level previously in the SCN, we used whole-cell patch-clamp recording to determine the cellular mechanisms of cannabinoid action on SCN neurons.

Received Nov. 23, 2009; revised June 10, 2010; accepted June 17, 2010.

Grant support provided by National Institutes of Health Grants NS34887, NS48476, NS 067409, and MH62335. We thank J. N. Davis for technical help.

Correspondence should be addressed to Anthony N. van den Pol, Department of Neurosurgery, Yale University, New Haven, CT 06520. E-mail: anthony.vandenpol@yale.edu.

DOI:10.1523/JNEUROSCI.5838-09.2010

 0270-6474/10/3010061-06$15.00/0

Materials and Methods

Electrophysiology

Experiments were performed in 15- to 30-d-old black Swiss mice ($n = 33$; >80 neurons) maintained in 12 h light/dark (LD) cycles (lights on at 7:00 A.M.) with food and water *ad libitum*. All recordings were done between 12:00 and 6:00 P.M.

Mice were anesthetized (sodium pentobarbital, 100 mg/kg), and the brains were removed and placed in ice-cold oxygenated (95% O_2, 5% CO_2) high-sucrose solution that contained the following (in mM): sucrose, 220; KCl, 2.5; $MgCl_2$, 6; $CaCl_2$, 1; NaH_2PO_4, 1.25; $NaHCO_3$, 26; glucose, 10. The anterior hypothalamus was gently excised and transferred to a Vibratome where 200–300 μm coronal slices were obtained. In some experiments we performed optic nerve stimulation using horizontal slices from the ventral hypothalamus (Pickard et al., 1999). Sections containing the SCN/retinohypothalamic axons were then moved to a custom chamber filled with normal ACSF containing the following (in mM): NaCl, 124; KCl, 3; $MgCl_2$, 2; $CaCl_2$, 2; NaH_2PO_4, 1.23; $NaHCO_3$, 26; glucose, 10. Tissue was maintained there at room temperature for 1–2 h and then transferred to a recording chamber mounted on a BX51WI Olympus upright microscope equipped with IR-DIC and fluorescence capabilities. All recordings were done near 35°C using a dual channel heat controller (Warner Instruments Inc).

Whole-cell recordings were performed with 5–7 MΩ glass pipettes pulled with a PP-83 vertical puller (Narishige) and filled with an internal solution containing the following (in mM): 130 $KMeSO_4$ (or KCl for IPSCs), 1 $MgCl_2$, 10 HEPES, 1.1 EGTA, 2 Mg-ATP, 0.5 Na_2-GTP, and 10 Na_2-phosphocreatin, pH 7.3 with KOH. SCN neurons were visually identified and approached with recording electrodes to achieve cell-attached configuration. Whole-cell mode was obtained after gentle application of negative pressure through the recording pipette and capacitive components were automatically compensated using Pulse

software (Heka Elektronik). The recordings were made using an EPC9 amplifier (HEKA Elektronik). Drugs were bath applied unless otherwise specified. AP5, CNQX, and bicuculline were from Tocris Bioscience and Sigma.

Retinohypothalamic axons were stimulated (50–100 μA, 0.2–0.5 ms, 0.1–0.2 Hz) with a bipolar electrode (World Precision Instruments) placed 0.5–1 mm away from recorded cells. In transverse slices, the stimulating electrode was positioned in the distal end of the optic chiasm. In some experiments we used horizontal slices to better preserve optic nerves (Pickard et al., 1999). In these cases, the stimulating electrode was placed in proximal optic nerves. As we did not observe major differences in evoked postsynaptic potentials between these two preparations, these data were pooled. All these recordings were done with 30 μM Bic in the bath to eliminate GABA-A receptor-mediated synaptic transmission.

For data analysis, PulseFit 8.54 (HEKA Electronik), Axograph 4.7 (Molecular Devices), and Igor Pro 4.07 (WaveMetrics) software were used. Spontaneous synaptic currents were detected using Axograph software as previously reported (Gao and van den Pol, 2001). Data are expressed as mean ± SEM. For statistical analysis we used one-way ANOVA. $p < 0.05$ was considered statistically significant.

Immunocytochemistry and RT-PCR

Rabbit antisera against CB1R (kind gift from Dr. K. Mackie, Indiana University, Bloomington, IN) (described by Twitchell et al., 1997; Tsou et al., 1998) used at 1:2000 together with goat anti-rabbit conjugated to red Alexa 594 was used to immunostain sections from paraformaldehyde perfusion-fixed GAD67-GFP knock-in mice that expressed green GFP selectively in GABAergic neurons (Tamamaki et al., 2003; Acuna-Goycolea et al., 2005); 15–25 μm thick coronal sections were cut on a cryostat. For RT-PCR experiments, coronal brain slices (300 μm) were microdissected to collect same-size tissue samples from the suprachiasmatic nucleus and cortex. Total RNA was isolated using the RNeasy Micro Kit (Qiagen). Reverse transcription was performed using the SuperScript III RT Kit (Invitrogen) and PCR was performed using the Expand High-Fidelity PCR Kit (Roche Diagnostics). The PCR primers were designed to yield a 523 bp product spanning nucleotides 420–942 of the mouse β-actin cDNA sequence (NM_007393) and a 244 bp product spanning nucleotides 415–658 of the mouse CB1R cDNA sequence (NM_007726) from GenBank. Both the β-actin and CB1R primer sets were designed to span introns of 0.5 and 18.4 kb, respectively. The primer sequences and conditions used were as follows: β-actin: 56.7°C annealing temp; 35 cycles; forward primer 5′-GCC AAC CGT GAA AAG ATG AC-3′; reverse primer 5′-CAA CGT CAC ACT TCA TGA TG-3′. CB1R: 57.4°C annealing temp; 35 cycles; forward primer 5′-GCA GAG CTC TCA TAG AGT CTG G-3′; reverse primer 5′-CAC GTA GAG GAG GTC TGT GGT G-3′. RT-PCR products were visualized on a 1.5% agarose electrophoresis gel.

Circadian rhythms

Cannulation and infusion. Adult (8- to 12-week-old) male C57BL/6J mice were anesthetized with intraperitoneal ketamine (91 mg/ml) and xylazine (9 mg/ml). Mice were placed in the stereotaxic apparatus (Cartesian Research) and the coordinates: posterior = 0.3 mm from bregma, lateral = 1.3 mm from the midline and dorsoventral = −2.2 mm from dura with head level were used to implant the tip of a 24-gauge guide cannula in the lateral ventricle (Butcher et al., 2002). Cannulas were secured in the skull with dental cement and a 30-gauge plug was placed in the cannula. Correct placement was confirmed by the observance of CSF welling from the guide cannula upon plug withdrawal. Following surgery animals recovered for 2 weeks. For infusions, mice were removed from the running wheel chambers, and a 30 gauge stainless steel injector needle was placed in the guide cannula. For the single-infusion paradigm, mice were infused (3 μl) with vehicle (DMSO), WIN55,212,2 (Tocris Bioscience) (WIN55; 3 nM/μl: 3 μl total volume) or AM251 (Tocris Bioscience; 3 nm/μl: 3 μl total volume) at a rate of 0.40 μl/min. For the double infusion paradigm, mice were initially infused with AM251 (6 nM/μl: 1.5 μl total volume), followed 15 min later with infusion of WIN55 (6 nM/μl: 1.5 μl total volume). After infusion, the plug was inserted back in the cannula and animals were returned to their running wheel chambers. Infusions were performed under dim light (15 W: < 1 lux at cage level) using a red safelight (Kodak filter: series 2).

Circadian activity protocol. Mice were individually housed and entrained to a 12 h LD cycle for 2 weeks; illumination (~100 lux at mid-cage level) was provided from a fluorescent white bulb. Mice were then transferred into continuous darkness (DD). During the DD period, mice received a weekly food and water replenishment at varying times during the subjective night. During cage maintenance, mice were exposed to a dim red light. Circadian behavior was monitored with a micro-switch attached to a 15 cm diameter running wheel. Switch closures were recorded to a PC running Vital View (Minimitter Corp) data acquisition software.

For all single-infusion experiments, animals were infused at circadian time (CT) 15.5 and exposed to white light (50 lux, 10 min) at CT 16. For the double infusion assay (AM251 and WIN55), the initial AM251 infusion was performed at CT 15.5, and the second WIN55 infusion was performed 15 min later. Mice were exposed to at least two of the infusion paradigms. Control mice not exposed to light went through the same handling protocol as the light-treated mice. Animals were maintained under DD throughout the experimental period and each infusion was separated by a 9–12 d period.

Assessment of light-induced phase-shifts. The linear regression method was used to assess the effects of light on clock phase. Thus, locomotor data were plotted as an actograph and a regression line was fitted by eye through the start of the subjective nighttime bout of activity for the 6 d period preceding light treatment. This line was projected through the period following light exposure. A second regression line was generated for days 3–8 following light administration. The difference in the projected versus the actual activity onset following light exposure was the phase shift. Data are expressed as mean phase shift ± SEM for each group and significance was assessed using the two-tailed Student's *t* test.

The Yale University or Ohio State University Animal Use Committee approved all animal procedures.

Results

Cannabinoids reduce light-evoked phase shifts

To assess the effects of cannabinoids on clock entrainment, dark-adapted mice were infused with WIN55 (9 nM) or with drug vehicle via an intraventricular cannula (Butcher et al., 2002; Cheng et al., 2006) and exposed to light (50 lux, 10 min) 30 min later (CT 16). Drug dose was based on work by other groups showing that the infusion of WIN55 in the low nanomole range (1–50) triggers dose-dependent neurophysiological effects (Martin et al., 1993). Locomotor activity, a read-out of clock phase, was used to monitor potential modulatory effects of WIN55. In vehicle infused control mice, photic stimulation led to a large and significant phase delay (~−140 min) in activity onset (Fig. 1*A*,*E*). In contrast, relative to vehicle infusion, cannabinoid receptor stimulation significantly reduced the phase-delaying effect of light (Fig. 1*A*,*E*, $p < 0.01$). To test the specificity of the modulatory effect of WIN55, mice were infused with the CB1R antagonist AM251 (9 nM) 15 min before WIN55 infusion. Under this double infusion paradigm, the WIN55-mediated depression of light-induced phase delays was partially reversed (Fig. 1*B*,*E*).

In the absence of photic stimulation, the activation of the CB1R via the infusion of WIN55 failed to significantly alter the clock free-running phase (Fig. 1*C*). Interestingly, inhibition of the CB1R via AM251 (9 nM) infusion triggered a modest, yet significant, phase delay of activity onset ($p < 0.05$, relative to vehicle infusion (Fig. 1*D*,*E*). Together, these data indicate that cannabinoid receptor activation markedly alters the capacity of light to entrain the core clock timing process and that release of endogenous cannabinoids (endocannabinoids) influences clock phasing.

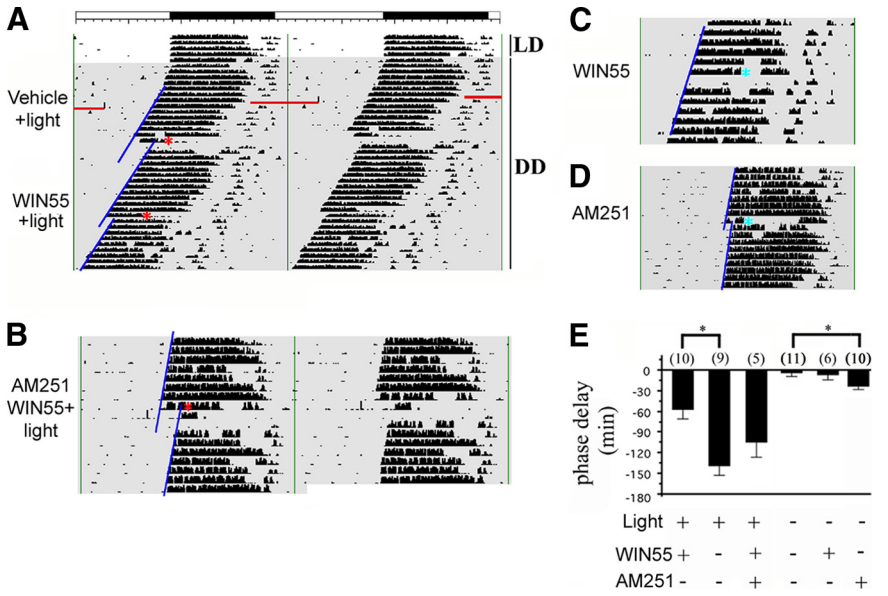

Figure 1. Cannabinoid receptor activation attenuates the phase-delaying effect of light. ***A***, Double plotted actograph showing the binned (5 min periods) wheel running activity of a representative mouse. This animal was initially maintained on a 12 h LD cycle, then transferred to total darkness (DD: grayed regions of the graph). After 2 weeks of free running, mice were infused with either drug vehicle (DMSO) or the WIN55 (9 nmol) 30 min before light (50 lux, 10 min) exposure at CT 16 (asterisk). Relative to the vehicle infusion, administration of WIN55 attenuated the phase-delaying effect of light. The horizontal red bar in the activity record denotes an "off-line" period when wheel-running activity was not recorded. ***B***, Mice were infused with AM251 (9 nmol) 15 min before WIN55 infusion and the phase shifting effect of light (50 lux, 10 min: asterisk) was evaluated. ***C***, ***D***, To determine whether cannabinoid receptor activation or inhibition altered timing in the absence of photic stimulation, mice were infused with WIN55 (***C***) or AM251 (***D***) at CT 15.5 (asterisks). Regression lines (blue) are provided to approximate potential stimulus-induced phase shifts. ***E***, The mean ± SEM phase-delaying effects of light under the various stimulus/infusion conditions are summarized. *$p < 0.01$ (significant): two-tailed Student's *t* test. Numbers above bars denote the number of mice for each condition.

Cannabinoids excite SCN neurons by a presynaptic mechanism

Both cell-attached and whole-cell recordings showed that SCN neurons spontaneously fire at ~4 Hz under control conditions and had a resting membrane potential of −56.4 ± 3.6 mV (range: −49 to −67 mV (Fig. 2*A*, top). Cannabinoids can reduce (Kreitzer and Regehr, 2001; Bacci et al., 2004; Heifets and Castillo, 2009; Kano et al., 2009) or increase firing rate or alter spike timing coordination (Robbe et al., 2006) in other brain regions. The CB1R agonist WIN55 (1–5 μM) increased SCN spike frequency (Fig. 2*A*, bottom; by 38.1 ± 5.8% [Range: 0.1–108.6%, $n = 8$] for cell-attached and by 56.7 ± 4.7% [Range: 0.2–145.2%, $n = 11$] for whole-cell recordings, $p < 0.05$). This increase in firing rate was generally accompanied by a slow depolarization (Fig. 2*B*, right, 5.9 ± 0.9 mV, $n = 11$, $p < 0.05$), and could be reversed to near control levels (93.5 ± 6.5% for spike frequency and 96.2 ± 6.7% for membrane potential, $n = 6$ for each case) by subsequent application of the CB1R antagonist AM251 (5 μM) following WIN55 washout. In addition, in the presence of AM251, WIN55 failed to depolarize SCN neurons and to increase their spike frequency (Fig. 2*B*, $n = 8$, $p = 0.68$), confirming that such a pharmacological manipulation resulted from specific activation of CB1Rs.

CB1Rs are often located in presynaptic structures (Glickfeld and Scanziani, 2006; Chevaleyre et al., 2007) and their activation regulates transmitter release. If WIN55-mediated enhancement of SCN neuronal activity were due to activation of presynaptic CB1R, an elimination of its actions after pharmacological blockade of GABA and glutamate synaptic inputs to these cells would be expected. We tested this possibility by using a solution consisting of ionotropic glutamate (50 μM AP5/10 μM CNQX) and GABA (30 μM Bicuculline: Bic) receptor antagonists in the external solution. Under these conditions, we did not find significant effects of WIN55 on SCN spike frequency or membrane potential ($n = 6$, Fig. 2*B*). These results suggest that the cannabinoid-mediated increase in activity is mainly dependent on the modulation of synaptic input. As the cannabinoid receptor agonist WIN55 increased action potential frequency of SCN neurons, we hypothesized that its effects were mostly mediated by a reduction of GABAergic tone (Glickfeld and Scanziani, 2006; Chevaleyre et al., 2007). This was directly tested in an additional set of experiments where WIN55 actions were evaluated in the presence of the GABA-A blocker Bic (30 μM). Under these conditions, WIN55 failed to affect SCN neuron spiking (change in firing: 3.3 ± 5.7%, change in membrane potential: 0.2 ± 1.1 mV) (Fig. 2*B*, $n = 7$). In addition, application of 30 μM Bic alone to SCN neurons mimicked WIN55 effects on spike frequency (Fig. 2*B*, left, increase in firing rate: 78.8 ± 5.6%, $n = 8$, $p < 0.01$) and membrane potential (Fig. 2*B*, right, depolarization 6.3 ± 2.3 mV, $n = 8$, $p < 0.05$), further suggesting that CB1R agonist actions on SCN neuronal activity were mediated by a reduction in GABA release.

To study this hypothesis more directly, we performed whole-cell recording experiments using high chloride electrodes that allowed detection of GABA-mediated inhibitory activity at physiological membrane potentials. Under control conditions, the mean IPSC frequency was 6.3 ± 0.9 Hz with a mean amplitude of 107.6 ± 14.7 pA (Fig. 2*C*, left, $n = 8$). WIN55 reduced the frequency of ISPCs by 47.6 ± 8.6% compared with controls (Fig. 2*C*,*D*, gray bars, $n = 9$, $p < 0.05$). ISPC amplitude was not significantly affected by CB1R agonists (Fig. 2*D*, black bars). These actions of WIN55 were due to selective modulation of CB1R, as they were not observed when the slices were pretreated with the CB1R antagonist AM251 (Fig. 2*D*). We also evaluated the possibility that SCN neurons may release endocannabinoids upon depolarization that in turn could retrogradely regulate synaptic inputs to SCN cells, as observed in other brain regions (Kreitzer and Regehr, 2001). Strong depolarizing stimuli were delivered to the soma of 11 SCN cells through the recording pipette (−70–0 mV, 5 s), and the frequency and amplitude of inhibitory activity was evaluated before and after such depolarization. Although there was a trend for a reduction in IPSC frequency (to 88.5 ± 12.5%), this was not statistically significant ($p = 0.25$). Similarly, the amplitude of inhibitory events was not significantly affected by postsynaptic depolarization (96.4 ± 8.6 from control, $p = 0.47$). Thus, under our experimental conditions we did not observe robust endocannabinoid release from SCN cells. In contrast, exogenous activation of CB1R consistently reduced the GABAergic synaptic tone to these neurons.

To determine whether CB1R activation selectively alters the release of GABA from presynaptic axons innervating SCN neurons, we recorded miniature (m)IPSCs in 0.5 μM tetrodotoxin. The frequency of mIPSCs was decreased by 52.3 ± 13.6% by WIN55 (Fig. 2*E*,*F*, gray bars, $n = 8$, $p < 0.05$). This effect was

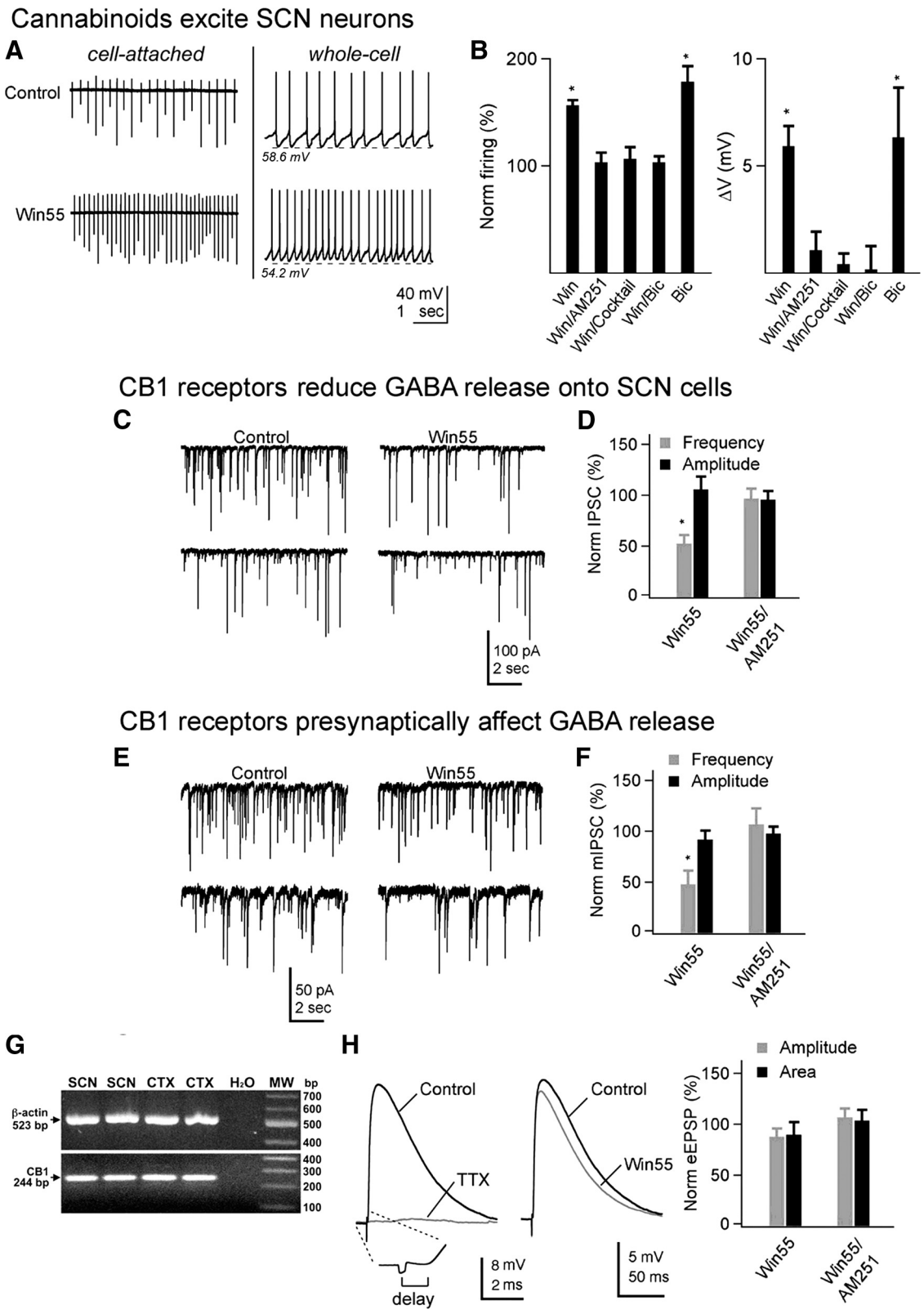

Figure 2. Cannabinoids excite SCN neurons by a presynaptic mechanism. ***A***, Cell-attached (left) and whole-cell (right) recordings from two representative SCN cells in control conditions (top) and in the presence of the cannabinoid agonist WIN55 (1–5 μM, bottom). Resting membrane potential before and after WIN55 is indicated for whole-cell recordings. Identical results were found in GFP expressing GABA cells from a GAD67-GFP mouse, and from a nontransgenic mouse; data are therefore pooled. ***B***, Summarized changes in the firing rate (left) and membrane potential (right) of SCN neurons under different experimental conditions (see Results). ***C***, ***D***, Representative records (***C***) and summary bar graph (***D***) showing the actions of cannabinoid agonist/antagonist on the frequency (gray) and amplitude (black) of IPSCs recorded in SCN neurons. ***E***, ***F***, Cannabinoid actions on miniature GABAergic currents recorded in the presence of TTX in a representative SCN neuron (***E***) or summarized for 8 experiments (***F***). ***G***, RT-PCR showing that microdissected SCN and control cortex (cortex—CTX) express CB1R mRNA (244 bp), whereas the water control lane was negative, as expected. ***H***, left, EPSPs recorded in a typical SCN cell following extracellular stimulation of the RHT. The enlarged area (left) shows the near 2 ms delay between the stimulus artifact and postsynaptic response (scale bars on the left belong to the enlarged area only). The mean of 10 trials before and after TTX (left) as well as before and after WIN55 (right) are shown for this (*Figure legend continues*.)

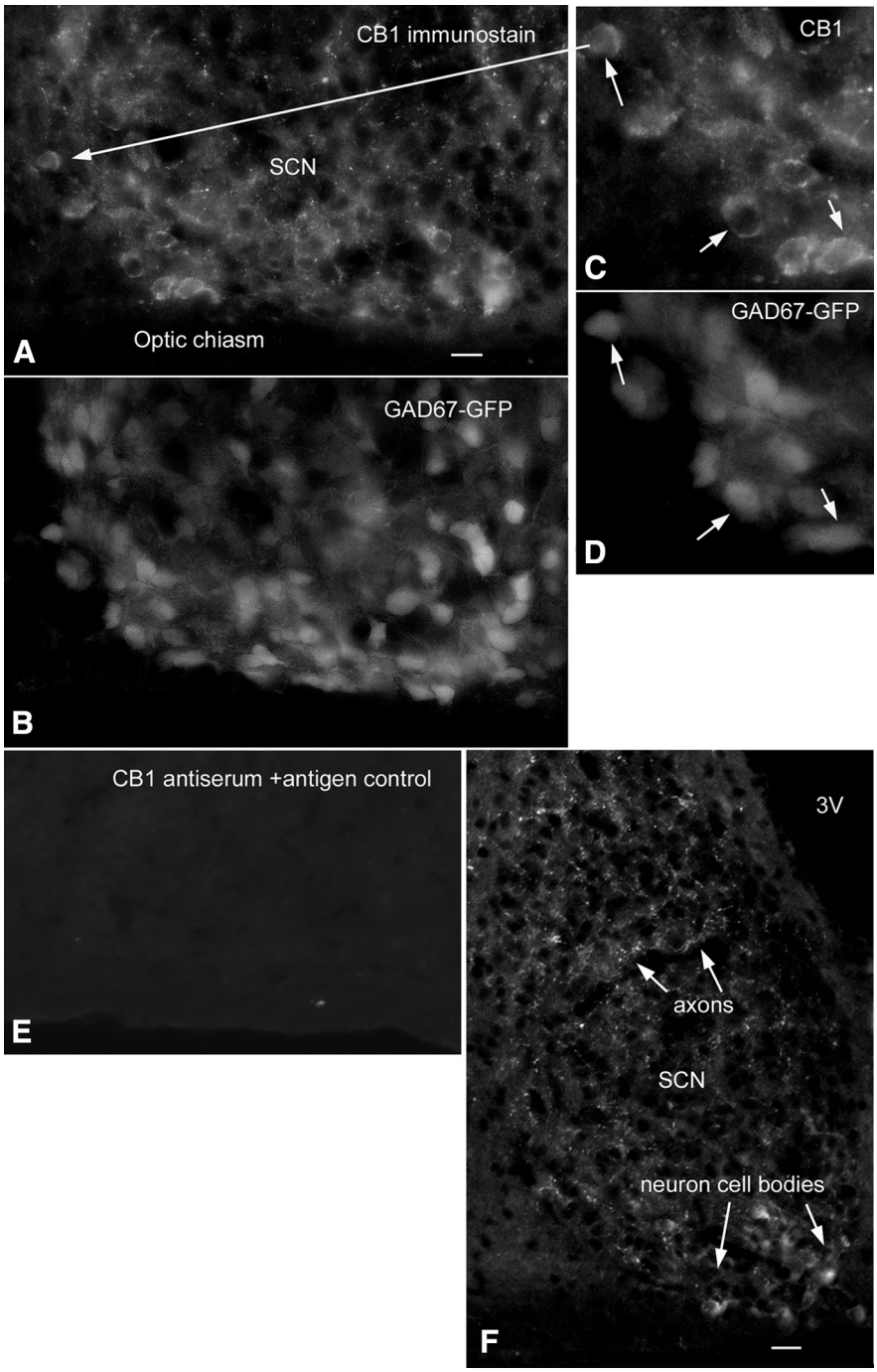

Figure 3. Cannabinoid receptor expression within the SCN. ***A***, Micrograph of ventral SCN showing CB1R immunostaining. Scale bar, 12 μm. ***B***, Same field as in ***A***. GABAergic neurons are identified by selective GFP expression in GAD67-GFP knock-in mice. ***C*** and ***D*** show higher magnifications of CB1R and GAD67-GFP, with arrows showing GABA cells that express CB1R immunoreactivity. Neurons that are GABAergic and express CB1R are shown with arrows. ***E***, Preincubation of CB1R antigen with the antiserum blocked SCN immunostaining. ***F***, Low-magnification micrograph showing CB1R immunostaining in the SCN. Cell bodies expressing CB1R immunofluorescence are found in the ventral SCN, axonal processes are found in ventral and dorsal (arrows) SCN. Scale bar, 30 μm.

prevented by AM251. The amplitude of these miniature inhibitory currents showed no significant change with WIN55 (Fig. 2*F*, black bars). Together, our results support the idea that presynaptic CB1R activation decreases GABA release from axonal boutons innervating SCN cells, releasing them from tonic inhibition and thereby increasing spike frequency. Given the high level of local circuit axons in the SCN (van den Pol, 1980) the CB1R could be on SCN axons, as suggested by our detection of CB1R mRNA in SCN neurons (Fig. 2*G*), or could originate from other loci that express CB1R (Herkenham et al., 1991).

To directly test whether local SCN GABAergic neurons and axons within the SCN express detectable CB1R we performed immunocytochemistry in hypothalamic sections from knock-in mice ($n = 3$) that expressed GFP under control of the GAD67 promoter selectively in GABA neurons (Fig. 3) (Tamamaki et al., 2003; Acuna-Goycolea et al., 2005), and from nontransgenic mice ($n = 3$). Strikingly, immunoreactivity for CB1R was localized in GABA neurons in the ventral SCN (Fig. 3*A–D*). Immunoreactive axons and boutons were found throughout the SCN, with the greatest density in the dorsolateral region (Fig. 3*F*). Addition of CB1R antigen to the antiserum before immunostaining blocked SCN immunostaining (Fig. 3*E*). Thus, a subset of ventral SCN neurons expresses CB1R.

Ventral SCN neurons are excited by retinal ganglion cells via the retinohypothalamic tract (RHT) (Kim and Dudek, 1991; Abrahamson and Moore, 2001) and we asked whether cannabinoids regulate RHT-SCN transmission. Electrical stimulation of the RHT (in coronal or horizontal slices, see Materials and Methods) evoked 5–12 mV EPSPs in ventral SCN neurons maintained at slightly hyperpolarized potentials by constant injection of negative current (Fig. 2*H*). WIN55 had little effect on the amplitude (decreased by 12.5 ± 7.8% [9.4 ± 6.5% decrease for 3 cells recorded in horizontal slices, 15.6 ± 8.4% decrease for the 3 neurons recorded in transverse slices], $n = 6$, $p > 0.05$) or time-voltage integral of EPSPs evoked by RHT stimulation (10.4 ± 12.5%, $n = 6$, $p > 0.05$) (Fig. 2*H*, right). Control application of glutamate receptor antagonists AP5 (100 μM) and CNQX (10 μM) blocked the EPSP by 96.2 ± 4.3%, consistent with RHT glutamate release (Kim and Dudek, 1991). Tetrodotoxin (0.5 μM) blocked the evoked EPSP by 97.5 ± 3.6%, supporting the view that the effect was dependent on action potentials (Fig. 2*H*, left). Thus cannabinoids do not appear to modulate retinal input to the SCN clock.

←

(*Figure legend continued.*) representative experiment. Scale bars on right are associated with full-traces in Figure 2 h. ***H***, right, Summary graph for the EPSP amplitude (gray) and area (black) in control, WIN55, and WIN55/AM251 (5 μM) conditions in 6 experiments. ***B***, Cocktail mixture solution: 50 μM AP5/10 μM CNQX/30 μM bicuculline (Bic). *$p < 0.05$.

Discussion

Our data show that cannabinoids alter the ability of the SCN clock to entrain to environmental light cues. This modulatory effect appears to be mediated at the level of altered GABAergic communication within the SCN. This interpretation is consistent with work showing that local GABAergic transmission influences a number of processes which are key to clock timing, including cell-to-cell communication and coupling between different regions of the SCN (Liu and Reppert, 2000; Shirakawa et al., 2000).

At the cellular level, CB1R activation reduced the release of GABA from presynaptic axon terminals in the SCN. This reduction in inhibitory drive led to an increase in the activity of postsynaptic SCN neurons, due to release from the tonic inhibition generated by the persistent activation of GABA-A receptors. The cannabinoid actions observed here are likely due to a presynaptic mechanism of activation of CB1Rs located on GABA terminals, as suggested by the cannabinoid-mediated attenuation of frequency but not amplitude of GABA-dependent mIPSCs. CB1R expressing GABA axons may arise from nearby SCN inhibitory cells, as suggested by our RT-PCR and immunocytochemistry analysis.

Our data are consistent with previous reports that GABA serves primarily an inhibitory function in the SCN (Gribkoff et al., 2003), although some studies have claimed that GABA can be excitatory at some phases of the circadian cycle due to elevated intracellular Cl^- (Wagner et al., 1997). Thus the effects of CB1Rs on SCN circuit activity (i.e., activation or inhibition) may be dependent on the time-of-day. Importantly, CB1R stimulation did not affect the retinal signaling to SCN, thus indicating that photic information was effectively relayed to the SCN, and thus further supporting the idea that CB1R altered clock entrainment results from the modulation of SCN neuronal circuits. That the CB1R antagonist AM251 evoked a shift in the clock phase suggests that endocannabinoid activity may modulate clock function.

Together, the data presented here reveal an effect of cannabinoids on clock physiology, and in turn, raise the possibility that alterations in SCN timing may be one mechanism by which cannabinoids influence time perception, in addition to cannabinoid actions on other regions of the brain including cortex, hippocampus, or striatum.

References

Abrahamson EE, Moore RY (2001) Suprachiasmatic nucleus in the mouse: retinal innervation, intrinsic organization and efferent projections. Brain Res 916:172–191.

Acuna-Goycolea C, Tamamaki N, Yanagawa Y, Obata K, van den Pol AN (2005) Mechanisms of neuropeptide Y, peptide YY, and pancreatic polypeptide inhibition of identified green fluorescent protein-expressing GABA neurons in the hypothalamic neuroendocrine arcuate nucleus. J Neurosci 25:7406–7419.

Bacci A, Huguenard JR, Prince DA (2004) Long-lasting self-inhibition of neocortical interneurons mediated by endocannabinoids. Nature 431: 312–316.

Butcher GQ, Doner J, Dziema H, Collamore M, Burgoon PW, Obrietan K (2002) The p42/44 mitogen-activated protein kinase pathway couples photic input to circadian clock entrainment. J Biol Chem 277:29519–29525.

Cheng HY, Dziema H, Papp J, Mathur DP, Koletar M, Ralph MR, Penninger JM, Obrietan K (2006) The molecular gatekeeper Dexras1 sculpts the photic responsiveness of the mammalian circadian clock. J Neurosci 26:12984–12995.

Chevaleyre V, Heifets BD, Kaeser PS, Südhof TC, Purpura DP, Castillo PE (2007) Endocannabinoid-mediated long-term plasticity requires cAMP/PKA signaling and RIM1alpha. Neuron 54:801–812.

Gao XB, van den Pol AN (2001) Melanin concentrating hormone depresses synaptic activity of glutamate and GABA neurons from rat lateral hypothalamus. J Physiol 533:237–252.

Glickfeld LL, Scanziani M (2006) Distinct timing in the activity of cannabinoid-sensitive and cannabinoid-insensitive basket cells. Nat Neurosci 9:807–815.

Gribkoff VK, Pieschl RL, Dudek FE (2003) GABA receptor-mediated inhibition of neuronal activity in rat SCN in vitro: pharmacology and influence of circadian phase. J Neurophysiol 90:1438–1448.

Heifets BD, Castillo PE (2009) Endocannabinoid signaling and long-term synaptic plasticity. Annu Rev Physiol 71:283–306.

Herkenham M, Lynn AB, Johnson MR, Melvin LS, de Costa BR, Rice KC (1991) Characterization and localization of cannabinoid receptors in rat brain: a quantitative in vitro autoradiographic study. J Neurosci 11:563–583.

Kano M, Ohno-Shosaku T, Hashimotodani Y, Uchigashima M, Watanabe M (2009) Endocannabinoid-mediated control of synaptic transmission. Physiol Rev 89:309–380.

Kim YI, Dudek FE (1991) Intracellular electrophysiological study of suprachiasmatic nucleus neurons in rodents: excitatory synaptic mechanisms J Physiol 444:269–287.

Kreitzer AC, Regehr WG (2001) Retrograde inhibition of presynaptic calcium influx by endogenous cannabinoids at excitatory synapses onto Purkinje cells. Neuron 29:717–727.

Liu C, Reppert SM (2000) GABA synchronizes clock cells within the suprachiasmatic circadian clock. Neuron 25:123–128.

Martin WJ, Lai NK, Patrick SL, Tsou K, Walker JM (1993) Antinociceptive actions of cannabinoids following intraventricular administration in rats. Brain Res 629:300–304.

Moore RY, Lenn NJ (1972) A retinohypothalamic projection in the rat. J Comp Neurol 146:1–14.

Pickard GE, Smith BN, Belenky M, Rea MA, Dudek FE, Sollars PJ (1999) 5-HT1B receptor-mediated presynaptic inhibition of retinal input to the suprachiasmatic nucleus. J Neurosci 19:4034–4045.

Robbe D, Montgomery SM, Thome A, Rueda-Orozco PE, McNaughton BL, Buzsaki G (2006) Cannabinoids reveal importance of spike timing coordination in hippocampal function. Nat Neurosci 9:1526–1533.

Sanford AE, Castillo E, Gannon RL (2008) Cannabinoids and hamster circadian activity rhythms. Brain Res 1222:141–148.

Shirakawa T, Honma S, Katsuno Y, Oguchi H, Honma KI (2000) Synchronization of circadian firing rhythms in cultured rat suprachiasmatic neurons. Eur J Neurosci 12:2833–2838.

Tamamaki N, Yanagawa Y, Tomioka R, Miyazaki J, Obata K, Kaneko T (2003) Green fluorescent protein expression and colocalization with calretinin, parvalbumin, and somatostatin in the GAD67-GFP knock-in mouse. J Comp Neurol 467:60–79.

Tinklenberg JR, Roth WT, Kopell BS (1976) Marijuana and ethanol: differential effects on time perception, heart rate, and subjective response. Psychopharmacology 49:275–279.

Tsou K, Brown S, Sañudo-Peña MC, Mackie K, Walker JM (1998) Immunohistochemical distribution of cannabinoid CB1 receptors in the rat central nervous system. Neuroscience 83:393–411.

Twitchell W, Brown S, Mackie K (1997) Cannabinoids inhibit N and P/Q-type calcium currents in cultured rat hippocampal neurons. J Neurophysiol 78:43–50.

Valenti M, Viganò D, Casico MG, Rubino T, Steardo L, Parolaro D, Di Marzo V (2004) Differential diurnal variations of anandamide and 2-arachidonoyl-glycerol levels in rat brain. Cell Mol Life Sci 61:945–950.

van den Pol AN (1980) The hypothalamic suprachiasmatic nucleus of rat: intrinsic anatomy. J Comp Neurol 191:661–702.

van den Pol AN, Tsujimoto KL (1985) Neurotransmitters of the hypothalamic suprachiasmatic nucleus: immunocytochemical analysis of 25 neuronal antigens. Neuroscience 15:1049–1086.

Wagner S, Castel M, Gainer H, Yarom Y (1997) GABA in the mammalian suprachiasmatic nucleus and its role in diurnal rhythmicity. Nature 387:598–603.

Wittmann G, Deli L, Kallo I, Hrabovszky E, Watanabe M, Liposits Z, Fekete C (2007) Distribution of type 1 cannabinoid receptor (CB1)-immunoreactive axons in the mouse hypothalamus. J Comp Neurol 503:270–279.